Soft Matter

PAPER

View Article Online
View Journal

Cite this: DOI: 10.1039/d1sm00301a

Formation of giant polymer vesicles by simple double emulsification using block copolymers as the sole surfactant†

Mazarine Houbrechts,[ab] Lucas Caire da Silva, *[a] Anitha Ethirajan [bc] and Katharina Landfester *[a]

Received 26th February 2021,
Accepted 23rd March 2021

DOI: 10.1039/d1sm00301a

rsc.li/soft-matter-journal

Polymer vesicles that mimic the function of cell membranes can be obtained through the self-assembly of amphiphilic block copolymers. The cell-like characteristics of polymer vesicles, such as the core–shell structure, semi-permeability and tunable surface chemistry make them excellent building blocks for artificial cells. However, the standard preparation methods for polymer vesicles can be time consuming, require special equipment, or have low encapsulation efficiency for large components, such as nanomaterials and proteins. Here, we introduce a new encapsulation strategy based on a simple double emulsification (SDE) approach which allows giant polymer vesicles to be formed in a short time and with basic laboratory equipment. The SDE method requires a single low molecular weight block copolymer that has the dual role of macromolecular surfactant and membrane building block. Giant polymer vesicles with diameters between 20–50 μm were produced, which allowed proteins and nanoparticles to be encapsulated. To demonstrate its practical application, we used the SDE method to assemble a simple artificial cell that mimics a two-step enzymatic cascade reaction. The SDE method described here introduces a new tool for simple and rapid fabrication of synthetic compartments.

Introduction

Block copolymer vesicles are known for having robust membranes, which can withstand greater mechanical stress and harsher chemical environments than lipid-based membranes.[1,2] These enhanced properties are a result of the relatively high molecular weight of the block copolymers and their varied chemical properties which is made possible through synthetic polymer chemistry. Both the structure and functionality of polymer vesicles can be fine-tuned, making them an attractive framework for the assembly of functional compartmentalized systems.[3–5] In terms of size, vesicles can be classified as either small, with diameters in the hundreds of nm range, and giant (>1 μm). One application of giant polymer vesicles is as synthetic compartments for artificial cells and organelles. These synthetic compartmentalized cell mimics can reproduce simple biological behaviour and function.[6] For example, by encapsulating a nanoparticle photocatalyst into giant polymer vesicles we were able to create a synthetic organelle that can recycle a coenzyme using light as a trigger.[7] Encapsulation of small vesicles into larger ones has also been explored as synthetic cell-mimics with a multi-compartmentalized architecture.[8] Synthetic compartments are also employed in the engineering of molecular factories, membrane-bound micro-reactors that can be used to synthesize biochemicals.[9]

Giant vesicles are basic structural elements of artificial cells in which smaller compartments and other components can be integrated to create hierarchical cell-like architectures. Therefore, it is desirable that their formation does not represent a bottleneck in the assembly of compartmentalized systems. Ideally, the vesicle assembly method must be easy to be followed by non-experts, offer encapsulation capabilities and produce a large numbers of vesicles per batch in a short time.

However, the current techniques available for the fabrication of giant polymeric vesicles cannot fulfil all these requirements at once. Film-hydration, for example, is a method that can produce polymer vesicles *via* the hydration-induced self-assembly of block copolymer films.[10,11] The method can be easily performed with minimal equipment, but usually offers limited encapsulation efficiency for large biomolecules and colloids, such as proteins and nanoparticles.[12] Another well-established method to create polymer vesicles is microfluidics, known for its excellent control of vesicle size distribution and

[a] Physical Chemistry of Polymers, Max Planck Institute for Polymer Research, Ackermannweg 10, 55128 Mainz, Germany.
E-mail: landfester@mpip-mainz.mpg.de, silva@mpip-mainz.mpg.de
[b] Institute for Materials Research, Hasselt University, Wetenschapspark 1, 3590 Diepenbeek, Belgium
[c] IMEC Associated Lab IMOMEC, Wetenschapspark 1, 3590 Diepenbeek, Belgium

† Electronic supplementary information (ESI) available. See DOI: 10.1039/d1sm00301a

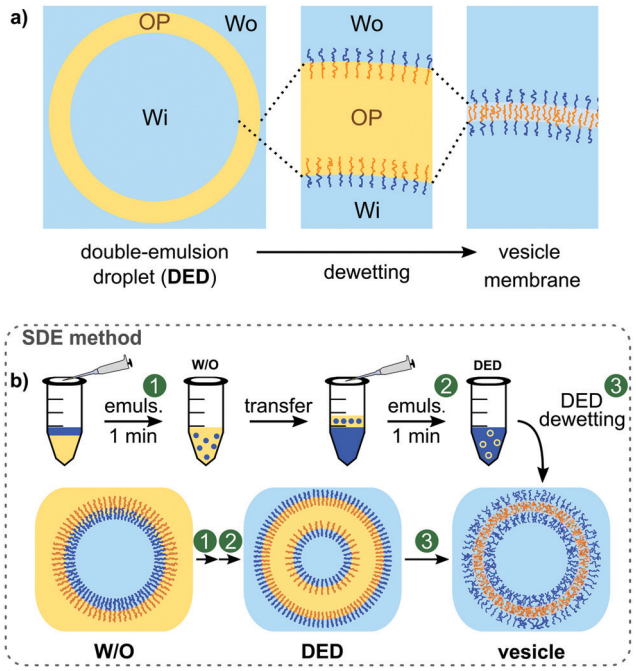

Scheme 1 (a) Steps during the formation of giant polymer vesicles starting with a single double emulsion droplet containing a dissolved block copolymer. The images show the evolution of the organic phase (OP) surrounded by the inner and outer water media (W). (b) Top: Description of each step of the single double emulsification method (SDE). The first emulsification (1) produces W/O droplets, which are re-emulsified (2) resulting in double emulsion droplets (DED). Vesicles are formed after DED dewetting (3), which involves phase separation induced by polymer self-assembly. Bottom: Cartoon showing the structure of the different emulsions and the resulting giant polymer vesicle.

high encapsulation efficiency.[13] However, this method requires special equipment and familiarity with the technique.[14]

Microfluidics is a powerful method because the vesicle self-assembly happens in well-defined single double emulsion droplets (DED), which act as templates for the vesicles. This is possible because the single DEDs have a water-in-oil-in-water (W/O/W) structure which is similar to that of giant diblock copolymer vesicles (Scheme 1a).

If an amphiphilic polymer is present in the oil phase (OP), displacement of the oil will trigger polymer self-assembly in the film. The result is a polymer membrane that retains the original vesicular shape of the original single DED. Unfortunately, formation of single DEDs is not a trivial task. Techniques such as microfluidics can achieve that efficiently by controlling the flows of the different phases through tiny channels that force the fluids to meet at the right place and time to form the droplets.[15]

Technically, the simplest way to form DEDs is by a conventional double emulsification method.[16] First, a W/O emulsion is created by mixing of an aqueous phase (W) and a hydrophobic phase (O) containing a lipophilic surfactant, which is needed for droplet stabilization. To form double emulsions, the W/O emulsion must be emulsified again. This time, the W/O dispersion is mixed with an aqueous solution that contains a hydrophilic surfactant, also needed for stabilization. Although this method is simple, it usually results in the formation of complex DEDs composed of multiple water droplets dispersed in a single oil droplet, which is itself dispersed in water.[17]

Complex DEDs cannot become giant polymer vesicles unless the internal water droplets are forced to coalesce, producing a single water core surrounded by a single oil film. This was demonstrated by Kim and Cheong by using a temperature responsive polymer to intentionally initiate the coalescence of internal water droplets in complex DEDs.[18] Although this approach is feasible, it requires special materials and conditions to force the complex DEDs to coalesce. The same work also describes the use of a block copolymer with the dual role of surfactant and vesicle membrane building block. Block copolymer surfactants have been mostly used for the formation of complex double emulsion droplets, leaving the possibility to create polymer vesicles by conventional emulsification mostly unexplored. For example, poly(styrene)-*block*-poly(ethylene oxide) has been employed as a single surfactant in a one-step formation of stable multiple emulsions.[19] Another example, from Hanson *et al.*, reports on the formation of nanoemulsions using block copolypeptides as the only surfactant in the system.[20]

Here, we demonstrate that single DEDs, and the polymer vesicles derived from them, can be directly formed using a simple double emulsification method (SDE), which is illustrated in Scheme 1b. Our method requires only one low molecular weight block copolymer that acts as the only surfactant for all emulsification steps, in addition to being the material from which the vesicle membranes are made.

Experimental

Materials

Albumin from bovine serum, fluorescein conjugate (BSA-FL, Invitrogen); amplex red™ (Sigma Aldrich); D-(+)-glucose (Sigma, ≥99.5% GC); fluorescein sodium salt (Fluka, standard); glucose oxidase from *Aspergillus niger* (GOx, type X-S, lyophilized powder, 100–250 units per mg, Sigma Aldrich); horseradish peroxidase (HRP, Type II, lyophilized powder, 150–250 units per mg, Sigma Aldrich); human serum albumin nanocapsules (d_H 240 nm) with encapsulated Vybrant™ DiO (provided by Natkritta Hüppe); poly(butadiene)-*block*-poly(ethylene oxide) (Polymer Source, Canada); sucrose (Sigma, ≥99.5% GC); toluene (Sigma-Aldrich, 99.9% HPLC).

Polymersome preparation using the SDE method

First, 5 μL of an aqueous sucrose solution (250 mM) was added into 30 μL of a toluene:PB–PEO solution (20, 10, 5 and 1 g L^{-1}) in a 1.5 mL microcentrifuge tube. This was followed by gentle emulsification for 1 min using a micropipette. DEDs were then formed by adding 5 μL of the W/O emulsion into 200 μL of an aqueous sucrose solution (250 mM), followed by another 1 min gentle emulsification step. The microcentrifuge tube containing the dispersion was left open to air for at least 2 hours. Finally,

100 μL of the dispersion was transferred into a microscope chamber slide containing 400 μL of aqueous glucose solution (250 mM) for further analysis. Micrographs of polymer vesicles were made on a Leica DMi8 Inverted Fluorescence Microscope.

Tensiometry

Interfacial tension (water/toluene) was measured on a DataPhysics SVT 20N tensiometer. The concentration of copolymers in toluene were 20.0 g L^{-1}, 10.0 g L^{-1}, 5.0 g L^{-1} and 1.0 g L^{-1}. All measurements were conducted at 22 °C with a rotation speed of 10 000 rpm. Interfacial tension data was determined using the Vonnegut method.

Encapsulation of materials into giant polymer vesicles

Different materials for encapsulation were first dispersed or dissolved in a sucrose solution (250 mM). 5 μL of this solution was used in the first emulsification step of the SDE method, which was then followed without further modifications. Polymer vesicles were observed by confocal laser microscopy (Leica TCS SP5, Wetzlar, Germany). The final concentrations present in the inner aqueous solutions were: GOx (0.05 mg mL^{-1}), HRP (0.05 mg mL^{-1}), HSA nanocapsules (2 mg mL^{-1}), BSA-FL (0.05–0.5 mg mL^{-1}). All aqueous solutions were prepared using deionized water from a Milli-Q purification system.

Determination of encapsulation efficiency

Vesicles containing the fluorescent tracer (BSA-FL) were prepared by first mixing 10 μL of BSA-FL (5 mg mL^{-1}, PBS buffer) in 50 μL aqueous sucrose (250 mM). This inner solution was then used for the subsequent steps of the SDE method, as described above. The composition of the aqueous solution in the final step was: 150 μL sucrose (250 mM), 50 μL glucose (250 mM) and 10 μL PBS buffer. The top 100 μL of the final dispersion was carefully transferred into a 96-well plate for fluorescence intensity measurements. Due to the density mismatch between the inner solution and the final continuous phase, the vesicles sank to the bottom of the centrifuge tube.

The bottom part of the dispersion (half of the total volume), which contained the vesicles, was sonicated, and pipetted constantly for 2 min to rupture all the vesicles and release the tracer into the continuous phase. Fluorescence intensity of the two parts was measured on a plate reader (Tecan M1000, λ_{Ex} = 490 nm; λ_{Em} = 520 nm) to determine the encapsulation efficiency (%EE):

$$\%EE = \frac{I_{rupt}}{I_{rupt} + 2I_{out}} \times 100\%$$

where I_{rupt} and I_{out} correspond to the fluorescence intensity of the bottom half containing the ruptured vesicles and the fluorescence intensity of the top half (no vesicles), respectively.

Results and discussion

The synthetic block copolymer poly(butadiene)$_x$-*block*-poly(ethylene oxide)$_y$ (PB$_x$-*b*-PEO$_y$) was chosen for the dual role of macromolecular surfactant and building block of the vesicle membranes. PEO is commonly used in materials that mimic glycoproteins in liposomes, imparting biocompatibility to the polymer membranes.[21,22] PB is a hydrophobic block with a low glass transition temperature, which produces flexible synthetic membranes.[23] In this work, we studied a total of three PB–PEOs with the distinct molecular weights and block structures shown in Fig. 1. The weight fraction of the hydrophilic block (PEO) was 33–34% (volume fraction 27–28%), which is compatible with the formation of polymer vesicles.[24]

Our first step was to determine the emulsifying properties of the different PB–PEOs by measuring the interfacial tension (σ) between water and the toluene solutions containing the polymers (Fig. 1). The data shows that the shortest copolymer, P1, was the best at lowering σ, with values falling under 1 mN m^{-1} for concentrations at or higher than 10 g L^{-1}. In contrast, polymers P2 and P3 provided a more modest decrease in σ, with values stabilizing at around 4–5 mN m^{-1}. As expected, σ decreased with increasing polymer concentration, because more surfactant was available to stabilize the liquid interface.

Lowering of σ, however, is limited by the ability of the copolymer to diffuse and adsorb at the interface. Longer polymer chains diffuse more slowly in diluted solution compared to short chain polymers.[25] This is the reason why P2 and P3, with the highest molecular weights, could not lower the interfacial tension below 4 mN m^{-1}.

Each polymer was evaluated as a surfactant to create the W/O emulsion. The emulsions were prepared by dispersing an aqueous solution into a toluene solution containing varying

polymer	BD, units	EO, units	M_n, g mol $^{-1}$
P1	22	14	2800
P2	74	45	6000
P3	113	73	9300

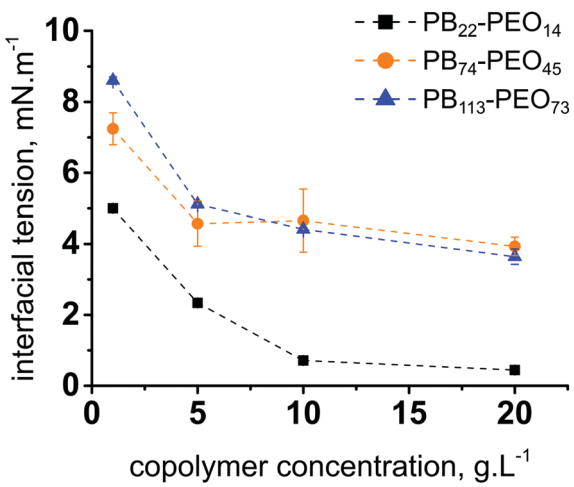

Fig. 1 Interfacial tension between water and toluene solutions containing different amounts of PB–PEO. BD: butadiene; EO: ethylene oxide. M_n: number average molecular weight. PDIs can be found in the ESI.†

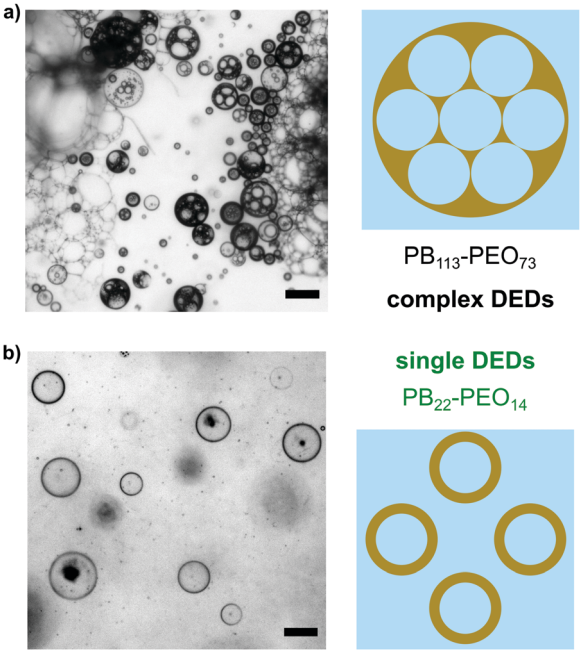

Fig. 2 Phase contrast micrographs of complex and single double emulsion droplets (DEDs) obtained with different polymers, P3 (20 g L^{-1}) and P1 (10 g L^{-1}), immediately after the second emulsification step. Scale bar: 100 μm.

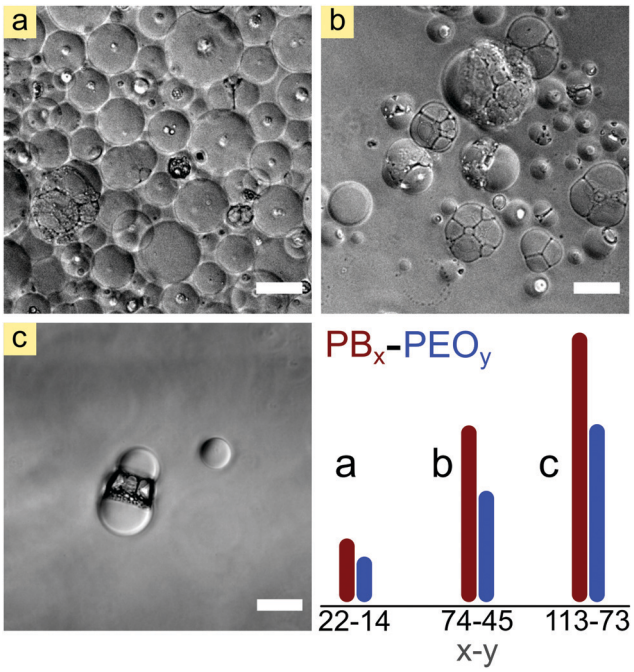

Fig. 3 Phase contrast micrographs of single vesicles and complex aggregates obtained with (a) P1, (b) P2 and (c) P3 at 20 g L^{-1}. Scale bars: 100 μm. The plot represents the relative length of each block in the different polymers, highlighting the short size of P1 compared to P2 and P3.

amounts of copolymer. The mixture was sheared by gentle pipetting for one minute. All three copolymers, P1–P3, produced W/O droplets that were stable for at least one hour (Fig. S1–S3, ESI†), which offered sufficient time for the next emulsification step to be performed. Fig. 2 shows images of the different types of DEDs (single or complex) obtained immediately after re-emulsification of the W/O droplets.

P3 produced mainly complex DEDs and oil droplets, indicating that this macromolecular surfactant offered only partial stabilization during DEDs formation. Single DEDs were produced with P1 (Fig. 2b). This polymer was surprisingly suited for both emulsification steps, producing single DEDs stabilized by steric repulsion between the PEG blocks.[26]

P2 showed intermediate behaviour, producing a mix of complex and single DEDs (Fig. S4, ESI†). Due to its shorter chains, P1 is expected to have a larger fraction of chains in solution which are not locked into micelles. These chains become available to adsorb at the oil–water interface, resulting in the higher performance of P1 compared to the other copolymers.

In contrast to complex DEDs, single DEDs are suitable templates for giant polymer vesicles. The polymer self-assembly that results in vesicles is initiated and sustained by the depletion of the organic phase in the DEDs. Depletion occurs mainly through a dewetting mechanism induced by the presence of a polymer excess in the DEDs.[27,28] Fig. 3 shows the different vesicle structures obtained for each polymer after toluene was removed from the DEDs. The single DEDs from P1 produced mainly single polymer vesicles. Complex aggregates became more significant with increasing the molecular weight of the polymer (Fig. S5, ESI†). Fig. 3 also suggests that the number of single vesicles significantly decreased with increasing the molecular weight of the polymers. To confirm that, the vesicle number densities, defined as the number of vesicles found per area (mm^2), were determined, and compared for each polymer. The results are shown in Fig. 4a.

A number density of zero vesicles was obtained for all polymers at a concentration of 1 g L^{-1}, irrespective of the molecular weight, indicating insufficient stabilization of the DEDs. For concentrations above 1 g L^{-1}, the highest number densities were obtained with P1, and the lowest, in fact essentially zero, was shown by P3. P2 showed intermediate behaviour, characterized by a lower number density than P1. Except for P3, there was a gradual increase in number density with increasing the polymer concentration.

Polymer type and concentration had a less striking effect on the average size of single polymer vesicles, as shown in Fig. 4b. In terms of size, all polymers and concentrations resulted in a broad size distribution with average vesicle diameters lying between 20 and 50 μm. P3 did not produce sufficient vesicles to enable determination of their size distribution.

The observed broad size distribution indicates that the vesicle formation by SDE is a rather complex process comprising distinct pathways that leads to vesicle formation. Large vesicles (up to 100 μm) are likely to result from initially complex DEDs that coalesce during the process.[29]

As the organic phase is depleted, the film that separates the original DEDs becomes thinner, increasing the likelihood of pore formation and coalescence.[30] The relatively uniform size distribution can be explained by vesicle budding. Vesicle membranes that

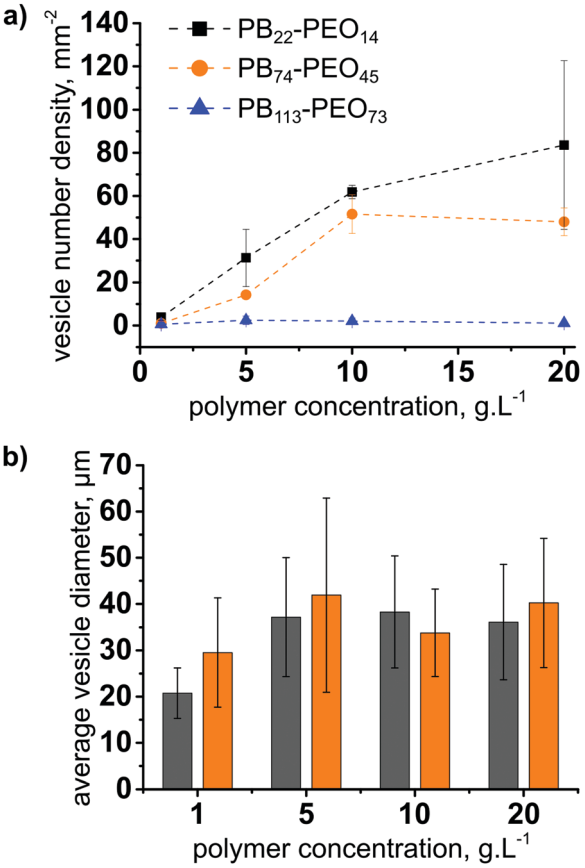

Fig. 4 (a) Vesicle number densities and (b) average vesicle diameter of single polymer vesicles obtained with the SDE method. Data were obtained by image analysis of 10 randomly picked frames (1.0 mm^2 area) from a total of 80 frames. Grey bars (P1), orange bars (P2).

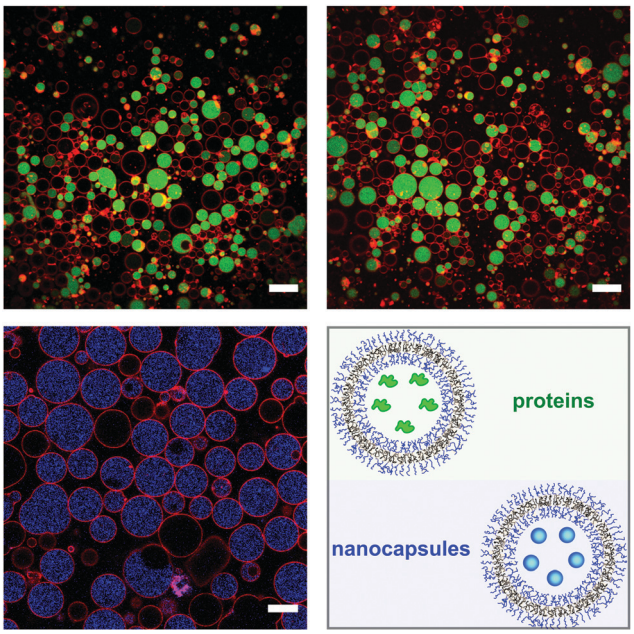

Fig. 5 Confocal fluorescence microscopy images of P1 vesicles containing the tagged protein BSA-FL (top row, green) and fluorescently labelled Human Serum Albumin nanocapsules. BSA-FL images are from independent samples with the same composition. The polymer membrane was stained with Nile Red. Scale bars: 60 µm (BSA-FL) and 25 µm.

contain an excessive amount of polymer can shed the excess by forming new vesicles. The polymer continues to self-assemble on top of the parent vesicles, resulting in relatively small vesicles with mean diameters of around 10 µm.[31]

Of all the polymers tested, P1 was the most efficient in terms of number of giant vesicles obtained. Polymer vesicles formed by other methods usually employ polymers that have a molecular weight that is higher than that of P1.[32] The low molecular weight allows P1 to efficiently replenish the new interfaces created in each step of the SDE method, explaining its excellent emulsifying power and overall performance.[33] Although P1 is a relatively short polymer, it has a molecular weight that is higher than that of typical lipids found in liposomes ($M_w < 1000$ g mol^{-1}). This guarantees the formation of robust DEDs that can survive the second emulsification step without emulsion breaking.[34]

Each polymer vesicle formed by the SDE method contains an aqueous core that is determined by the nature of the aqueous solution used in the first of the two emulsification steps. Therefore, materials that are either dissolved or dispersed in that aqueous phase will become encapsulated in the resulting polymer vesicles. Encapsulation of bio- and nano-materials in synthetic vesicles has become a powerful way to create simple artificial cells in the laboratory.[35–37] To demonstrate the encapsulation properties of the vesicles obtained by SDE, we encapsulated a model protein and nanocapsules into our P1 vesicles. Fig. 5 shows confocal microscopy images of polymer vesicles with the encapsulated materials. The images show that both materials could be efficiently encapsulated within the giant polymer vesicles, producing a high number of vesicles that contain the desired component. However, not all vesicles contain encapsulated materials in their core. Empty vesicles can be formed through budding since the content exchange between the source and daughter vesicles can be limited, especially for large payloads. Budding is usually triggered by a strain imposed on the membrane, which is more likely to happen during DED dewetting.[38,39]

To determine the encapsulation efficiency, P1 vesicles containing a protein tracer (BSA-FL) were prepared using the SDE method. The vesicles were mechanically ruptured by sonication and the amount of the tracer released after burst was compared to its total amount in the system. The results are shown in Fig. 6.

The average encapsulation efficiency (EE) was 21 ± 5%, which is comparable to the EE offered by techniques such as film hydration.[12,40] The EE is not higher because the DEDs and vesicles can burst during the dewetting stage.[28] Nevertheless, many giant vesicles (over 2000 per batch) encapsulating different materials can be obtained in just a few hours. These vesicles offer a unique opportunity for the convenient assembly of more complex compartmentalized systems, such as vesicle-based bioreactors, and artificial cells.[41,42]

To show the applicability of the SDE method, we used it to assemble a simple bioreactor that mimicks a two-step

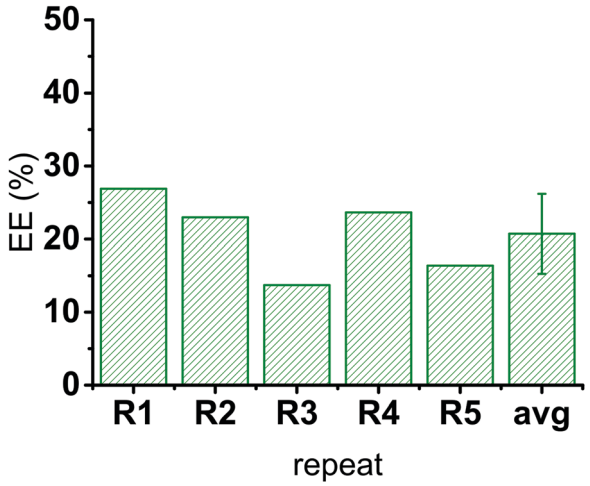

Fig. 6 Encapsulation efficiency (%EE) of P1 vesicles obtained with the SDE method. Determined by comparison between the presence of the BSA-FL tracer inside and outside the vesicles at the end of the procedure. Data corresponds to five repeats and an average value.

enzymatic cascade reaction (Fig. 7a). The reaction occurs inside the vesicles and is sustained by substrates present in the surrounding medium. The cascade reaction was mediated by two enzymes: glucose oxidase (GOx) and horseradish peroxidase (HRP), which work in tandem to oxidize a fluorogenic probe (Amplex™ Red).[43]

The bioreactors were created by encapsulation of the GOx and HRP in giant polymer vesicles using the SDE method. The reaction was started by addition of Amplex™ Red into the medium surrounding the bioreactors to a final concentration of 30 μM. First, β-D-glucose was oxidized by GOx, producing D-glucono-δ-lactone and hydrogen peroxide (H_2O_2). The H_2O_2 was then used by HRP to oxidize the colourless Amplex™ Red, which was able to cross the vesicle membrane, giving a highly fluorescent product that was detected by confocal laser microscopy (Fig. 7b). Plots of the normalized mean fluorescence intensity from different vesicles shows that the maximum signal intensities were reached between 100–150 s. Beyond this point, the FL intensity either remained constant, or decreased, which indicates leakage. In some cases, bursting was observed due to the rapid increase in osmotic pressure caused by the accumulation of reaction products inside the vesicles.[44]

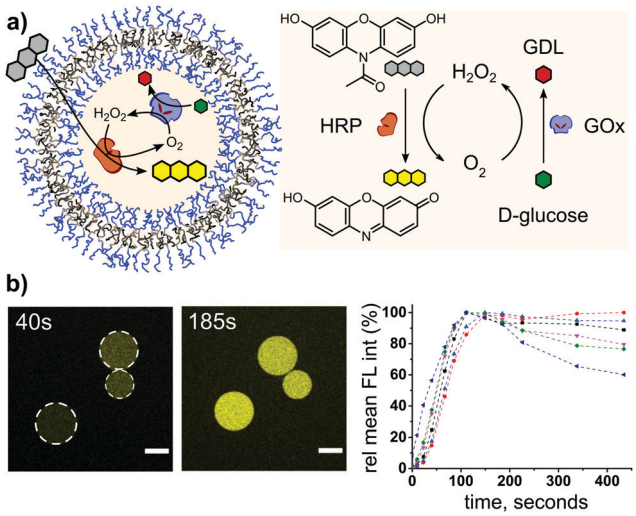

Fig. 7 (a) Scheme showing the enzymatic cascade reaction that occurs inside the polymer vesicles (bioreactors). HRP: horseradish peroxidase; GDL: glucono-delta-lactone; GOx: glucose oxidase. (b) Confocal microscope images of the bioreactors taken at different times from the reaction start. The plot shows the relative fluorescence intensity of the product over time.

Conclusions

In summary, the SDE method is a simple and efficient alternative for the formation of polymer vesicles and more complex compartmentalized systems. The method requires only basic laboratory equipment and can be easily reproduced by non-specialists. Our results suggest that low molecular weight block copolymers are required for SDE to work. This is because its low molecular weight allows the block copolymer to act as an efficient emulsifier for all the steps involved in the formation of the double emulsions. Although the SDE method does not produce vesicles with a narrow size distribution, a large number of vesicles can be easily obtained in just a few of hours.

Conflicts of interest

There are no conflicts to declare.

Acknowledgements

This work is part of the research conducted within the Max Planck Consortium for Synthetic Biology (MaxSynBio) jointly funded by the Federal Ministry of Education and Research of Germany (BMBF) and the Max Planck Society. We thank Natkritta Hüppe for providing the HSA nanocapsules and Tsvetomir Ivanov for Fig. S3 in the ESI.† Open Access funding provided by the Max Planck Society.

Notes and references

1 D. E. Discher and A. Eisenberg, *Science*, 2002, **297**, 967–973.
2 D. E. Discher and F. Ahmed, *Annu. Rev. Biomed. Eng.*, 2006, **8**, 323–341.
3 M. Marguet, C. Bonduelle and S. Lecommandoux, *Chem. Soc. Rev.*, 2013, **42**, 512–529.
4 C. E. Meyer, S. L. Abram, I. Craciun and C. G. Palivan, *Phys. Chem. Chem. Phys.*, 2020, **22**, 11197–11218.
5 D. Lensen, D. M. Vriezema and J. C. M. van Hest, *Macromol. Biosci.*, 2008, **8**, 991–1005.
6 M. Garni, R. Wehr, S. Y. Avsar, C. John, C. Palivan and W. Meier, *Eur. Polym. J.*, 2019, **112**, 346–364.
7 B. C. Ma, L. Caire da Silva, S. M. Jo, F. R. Wurm, M. B. Bannwarth, K. A. I. Zhang, K. Sundmacher and K. Landfester, *ChemBioChem*, 2019, **20**, 2593–2596.

8 R. J. R. W. Peters, M. Marguet, S. Marais, M. W. Fraaije, J. C. M. Van Hest and S. Lecommandoux, *Angew. Chem., Int. Ed.*, 2014, **53**, 146–150.
9 T. Einfalt, M. Garni, D. Witzigmann, S. Sieber, N. Baltisberger, J. Huwyler, W. Meier and C. G. Palivan, *Adv. Sci.*, 2020, **7**, 1901923.
10 L. Caire da Silva, E. Rideau and K. Landfester, *Macromol. Rapid Commun.*, 2019, **40**, 1–4.
11 E. Rideau, F. R. Wurm and K. Landfester, *Polym. Chem.*, 2018, **9**, 5385–5394.
12 A. Weinberger, F. C. Tsai, G. H. Koenderink, T. F. Schmidt, R. Itri, W. Meier, T. Schmatko, A. Schröder and C. Marques, *Biophys. J.*, 2013, **105**, 154–164.
13 D. T. Chong, X. S. Liu, H. J. Ma, G. Y. Huang, Y. L. Han, X. Y. Cui, J. J. Yan and F. Xu, *Microfluid. Nanofluid.*, 2015, **19**, 1071–1090.
14 C. S. Ho, J. W. Kim and D. A. Weitz, *J. Am. Chem. Soc.*, 2008, **130**, 9543–9549.
15 C. H. Choi, J. Kim, J. O. Nam, S. M. Kang, S. G. Jeong and C. S. Lee, *ChemPhysChem*, 2014, **15**, 21–29.
16 N. Garti, *Colloids Surf., A*, 1997, **123–124**, 233–246.
17 M. F. Ficheux, L. Bonakdar, F. Leal-Calderon and J. Bibette, *Langmuir*, 1998, **14**, 2702–2706.
18 M. R. Kim and I. W. Cheong, *Langmuir*, 2016, **32**, 9223–9228.
19 L. Z. Hong, G. Q. Sun, J. G. Cai and T. Ngai, *Langmuir*, 2012, **28**, 2332–2336.
20 J. A. Hanson, C. B. Chang, S. M. Graves, Z. Li, T. G. Mason and T. J. Deming, *Nature*, 2008, **455**, 85–88.
21 B. M. Discher, Y.-Y. Won, D. S. Ege, J. C.-M. Lee, F. S. Bates, D. E. Discher and D. A. Hammer, *Science*, 1999, **284**, 1143–1146.
22 T. Hellweg, Block copolymer surfactant mixtures in aqueous solution: Can we achieve size and shape control by co-micellization?, in *Self-Organized Nanostructures of Amphiphilic Block Copolymers II. Advances in Polymer Science. 242*, ed. A. H. E. Müller and O. Borisov, Springer-Verlag Berlin, Berlin, 2011, pp. 1–27.
23 S. So, L. J. Yao and T. P. Lodge, *J. Phys. Chem. B*, 2015, **119**, 15054–15062.
24 S. Jain and F. S. Bates, *Science*, 2003, **300**, 460–464.
25 R. M. Prokop, M. L. Hair and A. W. Neumann, *Macromolecules*, 1996, **29**, 5902–5906.
26 J. Israelachvili, *Proc. Natl. Acad. Sci. U. S. A.*, 1997, **94**, 8378–8379.
27 R. C. Hayward, A. S. Utada, N. Dan and D. A. Weitz, *Langmuir*, 2006, **22**, 4457–4461.
28 H. C. Shum, E. Santanach-Carreras, J. W. Kim, A. Ehrlicher, J. Bibette and D. A. Weitz, *J. Am. Chem. Soc.*, 2011, **133**, 4420–4426.
29 H. Chen, Y. Zhao, J. Li, M. Guo, J. Wan, D. A. Weitz and H. A. Stone, *Lab Chip*, 2011, **11**, 2312–2315.
30 H. Bermúdez, H. Aranda-Espinoza, D. A. Hammer and D. E. Discher, *Europhys. Lett.*, 2003, **64**, 550–556.
31 J. Thiele, V. Chokkalingam, S. Ma, D. A. Wilson and W. T. S. Huck, *Mater. Horiz.*, 2014, **1**, 96–101.
32 E. Rideau, R. Dimova, P. Schwille, F. R. Wurm and K. Landfester, *Chem. Soc. Rev.*, 2018, **47**, 8505–8970.
33 R. M. Prokop, M. L. Hair and A. W. Neumann, *Macromolecules*, 1996, **29**, 5902–5906.
34 K. Kamiya and S. Takeuchi, *J. Mater. Chem. B*, 2017, **5**, 5911–5923.
35 K. Y. Lee, S. J. Park, K. A. Lee, S. H. Kim, H. Kim, Y. Meroz, L. Mahadevan, K. H. Jung, T. K. Ahn, K. K. Parker and K. Shin, *Nat. Biotechnol.*, 2018, **36**, 530–535.
36 X. Liu, P. Formanek, B. Voit and D. Appelhans, *Angew. Chem., Int. Ed.*, 2017, **56**, 16233–16238.
37 P. Schwille, J. Spatz, K. Landfester, E. Bodenschatz, S. Herminghaus, V. Sourjik, T. Erb, P. Bastiaens, R. Lipowsky, A. Hyman, P. Dabrock, J.-C. Baret, T. Vidakovic-Koch, P. Bieling, R. Dimova, H. Mutschler, T. Robinson, D. Tang, S. Wegner and K. Sundmacher, *Angew. Chem., Int. Ed.*, 2018, **57**, 13382–13392.
38 R. Rodríguez-García, M. Mell, I. López-Montero, J. Netzel, T. Hellweg and F. Monroy, *Soft Matter*, 2011, **7**, 1532–1542.
39 G. P. Robbins, M. Jimbo, J. Swift, M. J. Therien, D. A. Hammer and I. J. Dmochowski, *J. Am. Chem. Soc.*, 2009, **131**, 3872–3874.
40 C. P. O'Neil, T. Suzuki, D. Demurtas, A. Finka and J. A. Hubbell, *Langmuir*, 2009, **25**, 9025–9029.
41 T. Trantidou, M. Friddin, Y. Elani, N. J. Brooks, R. V. Law, J. M. Seddon and O. Ces, *ACS Nano*, 2017, **11**, 6549–6565.
42 Y. Elani, R. V. Law and O. Ces, *Nat. Commun.*, 2014, **5**, 5305.
43 P. Lefrançois, B. Goudeau and S. Arbault, *Analyst*, 2020, **145**, 7922–7931.
44 A. Peyret, E. Ibarboure, A. Tron, L. Beaute, R. Rust, O. Sandre, N. D. McClenaghan and S. Lecommandoux, *Angew. Chem., Int. Ed.*, 2017, **56**, 1566–1570.